JACS
JOURNAL OF THE AMERICAN CHEMICAL SOCIETY

pubs.acs.org/JACS

Article

Mechanistic Studies of the Palladium-Catalyzed Desulfinative Cross-Coupling of Aryl Bromides and (Hetero)Aryl Sulfinate Salts

Antoine de Gombert, Alasdair I. McKay, Christopher J. Davis, Katherine M. Wheelhouse, and Michael C. Willis*

Cite This: J. Am. Chem. Soc. 2020, 142, 3564−3576

Read Online

ACCESS | Metrics & More | Article Recommendations | Supporting Information

ABSTRACT: Pyridine and related heterocyclic sulfinates have recently emerged as effective nucleophilic coupling partners in palladium-catalyzed cross-coupling reactions with (hetero)aryl halides. These sulfinate reagents are straightforward to prepare, stable to storage and coupling reaction conditions, and deliver efficient reactions, thus offering many advantages, compared to the corresponding boron-derived reagents. Despite the success of these reactions, there are only scant details of the reaction mechanism. In this study, we use structural and kinetic analysis to investigate the mechanism of these important coupling reactions in detail. We compare a pyridine-2-sulfinate with a carbocyclic sulfinate and establish different catalyst resting states, and turnover limiting steps, for the two classes of reagent. For the carbocyclic sulfinate, the aryl bromide oxidative addition complex is the resting state intermediate, and transmetalation is turnover-limiting. In contrast, for the pyridine sulfinate, a chelated Pd(II) sulfinate complex formed post-transmetalation is the resting-state intermediate, and loss of SO_2 from this complex is turnover-limiting. We also investigated the role of the basic additive potassium carbonate, the use of which is crucial for efficient reactions, and deduced a dual function in which carbonate is responsible for the removal of free sulfur dioxide from the reaction medium, and the potassium cation plays a role in accelerating transmetalation. In addition, we show that sulfinate homocoupling is responsible for converting $Pd(OAc)_2$ to a catalytically active Pd(0) complex. Together, these studies shed light on the challenges that must be overcome to deliver improved, lower temperature versions of these synthetically important processes.

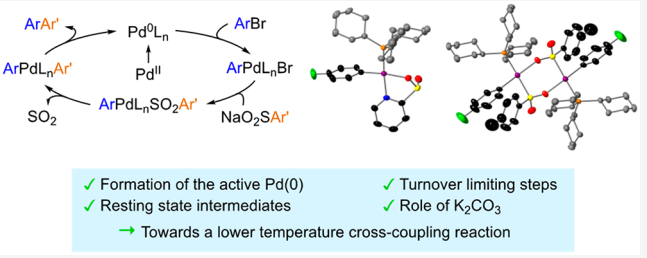

1. INTRODUCTION

The Suzuki−Miyaura reaction,[1] in which a boron-based coupling partner is combined with an aryl halide using a palladium catalyst, has revolutionized synthetic chemistry in the pharmaceutical industry.[2] However, applying these reactions to the preparation of heteroaromatic derivatives has long remained a challenge, because the corresponding heterocycle-derived boronic acids (and related boron-based reagents) can be challenging to prepare, unstable, base-sensitive, and prone to protodeboronation and decomposition under cross-coupling conditions. This is particularly true for pyridine and related diazene-derived boronic acids.[3] In this context, the Willis laboratory has recently reported the use of pyridyl[4] and heteroaryl[5] sulfinate salts as nucleophilic reagents in palladium-catalyzed cross-coupling reactions with aryl and heteroaryl halides (Scheme 1a). These sulfinate salts, several of which are now commercial products, are stable reagents and deliver efficient reactions with challenging coupling partners, thus addressing many of the limitations of their boron counterparts. More recently, the use of related heteroaryl allylsulfones, which function as latent sulfinate coupling partners, has also been reported.[6]

More generally, transition-metal-catalyzed desulfinative cross-coupling has emerged as an effective method for C−C bond formation.[7] First employed for homocoupling with stoichiometric palladium(II),[8] sulfinate salts can now be employed as the electrophilic coupling partner in Mizoroki−Heck,[9] Suzuki−Miyaura,[10] and Hiyama[11] cross-coupling processes. Their use as nucleophilic coupling partners was first reported in a 1992 patent,[12] before being more widely developed for both aromatic[13] or five-membered *O*- and *S*-heteroaromatic[14] systems. Catalytic versions of homocoupling reactions have also been reported.[15] Together with decarboxylation-based methods, desulfination can be considered as a potentially more sustainable approach to cross-coupling chemistry, relative to processes that require the preparation and use of costly and sensitive organometallic reagents. The release of SO_2 gas as the main byproduct should also be considered in this context. While decarboxylation has been

Received: December 9, 2019
Published: February 7, 2020

Scheme 1. Heterocyclic Sulfinate Coupling Reactions, a Generalized Mechanism, and Aims of the Study

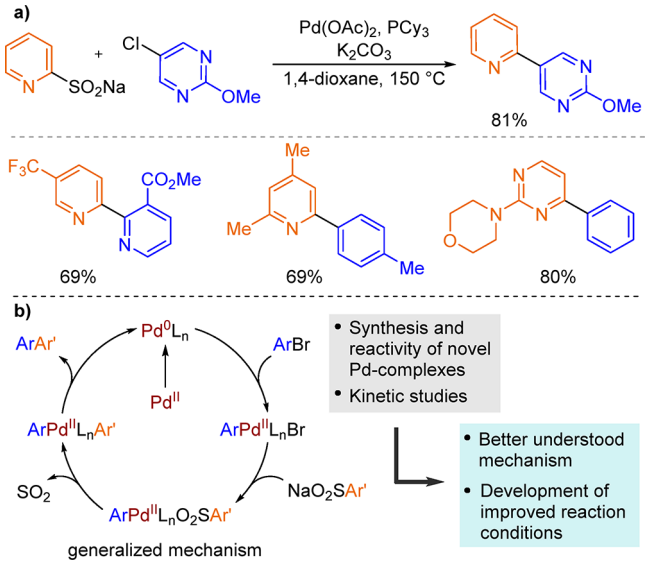

studied both experimentally[16] and theoretically,[17] the intrinsic difference between an sp^2-hybridized carbon center and an sp^3-hybridized sulfur center precludes direct transposition of these studies to the desulfinative variants. Similarly, although carbonylation and sulfur dioxide insertion are related processes, they can follow different mechanistic pathways.[18] To date, no mechanistic investigation of a desulfinative cross-coupling process using sulfinate salts as nucleophilic coupling partners has been reported.[19]

A generalized mechanism for desulfinative cross-coupling is shown in Scheme 1b. Reduction of the Pd(II) precatalyst to the active Pd(0) species is followed by oxidative addition of the carbon-bromide bond to the transition metal. Transmetalation between the alkali metal sulfinate salt and the oxidative addition complex generates a putative palladium sulfinate intermediate. Extrusion of SO_2 followed by reductive elimination regenerates the Pd(0) catalyst and delivers product. In the present study, we explore this mechanism using two model sulfinate reagents, allowing the comparison of carbocyclic and heterocyclic substrates. We describe the first synthesis, characterization, and reactivity study of the putative palladium sulfinate intermediates. Using a combination of stoichiometric experiments and kinetic studies, we propose different resting-state intermediates and turnover limiting steps for the two different classes of sulfinate reagent. We also investigate the role of the base, which is a crucial additive for reactivity. The aim of these studies was to improve the understanding of these synthetically important transformations, and also to provide insights for the development of reactions which proceed using milder conditions, particularly with regard to the high temperatures (120−185 °C) generally used in these reactions.[7]

2. RESULTS AND DISCUSSION

2.1. Model Reactions. The coupling of the unsubstituted sodium pyridine-2-sulfinate salt **1** with 1-bromo-4-fluorobenzene **2** proceeds in 95% yield as shown in Scheme 2. Although these reactions were initially developed for pyridine sulfinate salts,[4] before being extended to a larger class of heteroaromatic substrates,[5] they can also be applied to carbocyclic variants.

Scheme 2. Substrates and Reactions To Be Studied

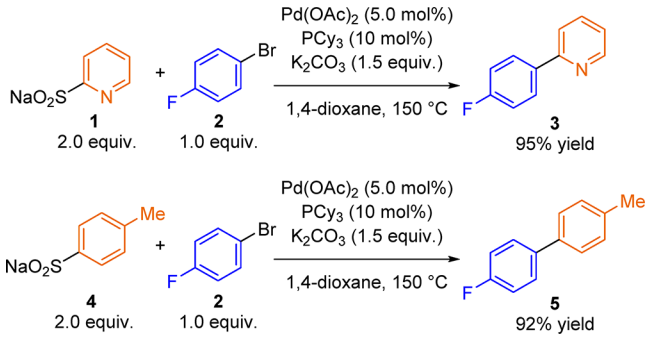

For example, sodium 4-methylbenzenesulfinate **4** can be combined with 1-bromo-4-fluorobenzene using $Pd(OAc)_2$, PCy_3, and K_2CO_3 at 150 °C to deliver the cross-coupling product **5** in 92% yield. Encouraged by the robustness of these reaction conditions, we chose to compare the reactivity of heterocyclic and carbocyclic sulfinate salts, as the carbocyclic variants of this cross-coupling also require high temperatures.[7] Indeed, such carbocyclic sulfinate salts are inexpensive, bench-stable reagents that can be easily prepared via a broad range of methods.[20] A lower temperature cross-coupling of such reagents would potentially establish sulfinates as attractive alternatives to the more-expensive boron-based reagents. Heterocyclic sulfinate **1** and carbocyclic sulfinate **4**, together with aryl bromide **2**, were therefore selected as the substrates for our proposed mechanistic study.

2.2. Synthesis and Characterization of Organometallic Intermediates. *2.2.1. Formation of the Active Palladium(0) Species.* Palladium(II) acetate is employed as the palladium source for these desulfinative cross-coupling reactions, and therefore the active Pd(0) species must be generated via a reductive process. This step is often overlooked in mechanistic studies, although the Pd(0) species could be generated from several different pathways and, thus, give rise to different kinetic profiles,[21] making the understanding of how Pd(0) is formed crucial for the design of accurate kinetic experiments (section 2.4). Phosphine oxidation has long been known as a pathway for palladium zero generation,[22] but nucleophilic coupling partners such as organolithium reagents,[23] organostannanes,[24] alcohols,[25] and amines[26] can also mediate the reduction of Pd(II) precatalysts. Having observed such reduction pathways, Buchwald and co-workers judiciously used substoichiometric amounts of an aryl boronic acid in order to ensure complete reduction of their Pd(II) precatalysts.[27] Furthermore, a synthetically useful dimerization of two sulfinate salts using stoichiometric amounts of Pd(II) was reported in the early 1970s.[8] Therefore, we examined the generation of the active catalyst in the presence of 4-methylbenzenesulfinate **4** (Figure 1). The two coupling partners 1-bromo-4-fluorobenzene **2** and 4-methylbenzenesulfinate **4** were introduced to a Young's NMR tube, together with K_2CO_3 and stoichiometric amounts of $Pd(OAc)_2$ and PCy_3 in a 2:1 ratio. The NMR tube was then gradually heated at different temperatures and the reaction was monitored by $^{31}P\{^1H\}$ and $^{19}F\{^1H\}$ NMR spectroscopy. The known $Pd(PCy_3)_2(OAc)_2$ complex[28] **6** was rapidly formed at room temperature. Upon heating to 60 °C, the $^{31}P\{^1H\}$ resonance of **6** started to decay to a broad signal at 29.83 ppm, corresponding to a set of broad doublets at 8.43 and 6.63

https://dx.doi.org/10.1021/jacs.9b13260
J. Am. Chem. Soc. 2020, 142, 3564−3576

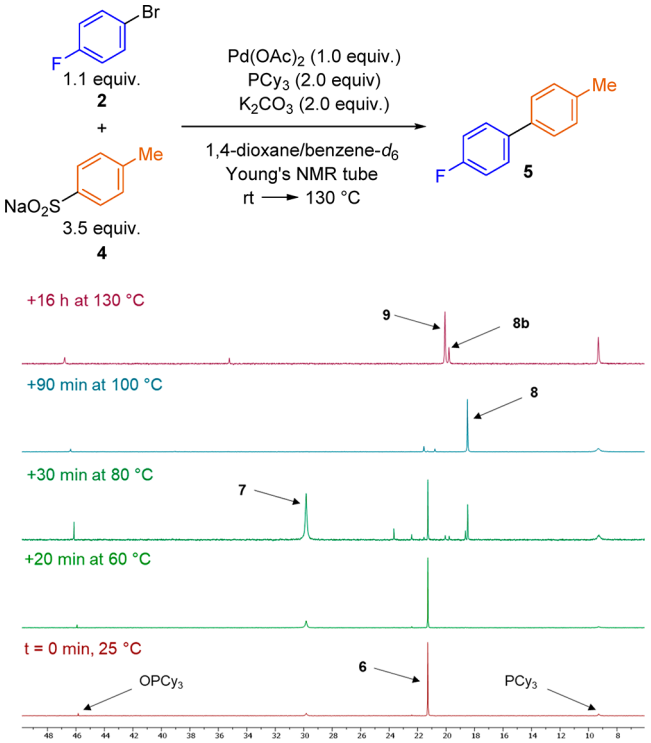

Figure 1. $^{31}P\{^{1}H\}$ NMR spectra of the reaction between Ar−Br (**2**) and Ar′SO_2Na (**4**) catalyzed by stoichiometric $Pd(OAc)_2$ and PCy_3 in a Young's NMR tube at various temperatures. [Legend: **6**, $Pd(OAc)_2(PCy_3)_2$; **7**, $(Ar'SO_2)Pd(PCy_3)_2(OAc)$; **8**, $(Ar')Pd(PCy_3)_2(OAc)$; **8b**, $(Ar')Pd(PCy_3)_2(Br)$; and **9**, $(Ar)(Pd)(PCy_3)_2(Br)$; Ar = 4-F-C_6H_4; Ar′ = 4-Me-C_6H_4.]

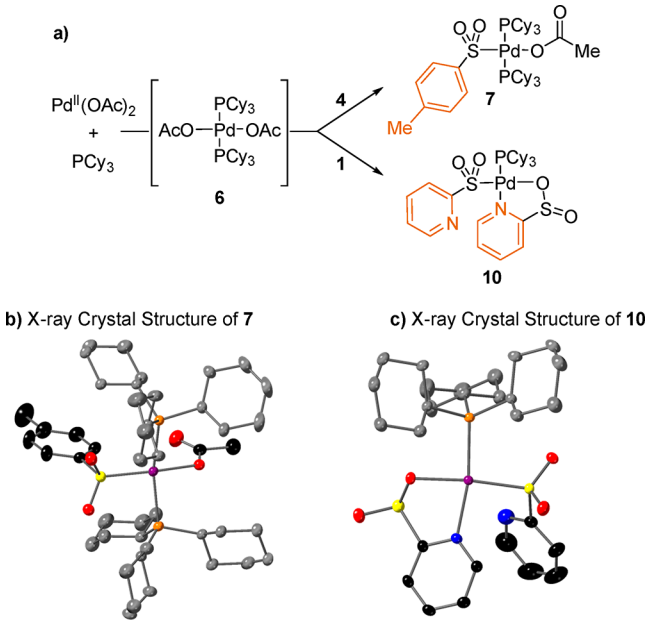

Figure 2. (a) Synthesis of the palladium sulfinate complexes **7** and **10**. X-ray crystal structures (50% displacement ellipsoids) of (b) **7** and (c) **10**. All H atoms have been omitted for the sake of clarity.

ppm in the ^{1}H NMR spectrum (see the Supporting Information (SI)).

The complex corresponding to these signals was isolated from a separate reaction that was performed for 16 h at 60 °C. Single crystals suitable for an X-ray diffraction (XRD) study were grown from CH_2Cl_2/hexane and revealed a sulfinato-*S* palladium complex **7** (Figures 2a and 2b). The structure displays a square planar geometry around the Pd center, with a trans arrangement of the phosphines. The Pd−S bond length of 2.2755(4) Å in **7** is shorter than those in (dppf)Pd(Me)(Cl)[29] and (BINAP)Pd($SO_2C_6H_4$Me)Cl[30] (2.3262(9) and 2.3331(7) Å, respectively). While the Pd−O bond length of 2.0975(13) Å is notably longer than that in $(PCy_3)_2$Pd$(OAc)_2$ (2.0288(17) Å), reflecting the strong trans influence of the sulfinate ligand. The arrangement of the acetate and the 4-methylbenzenesulfinate about the palladium affords a close contact (2.578(2) Å) between the nonbound O atom of the acetate and the 2-aryl-hydrogen of the 4-methylbenzenesulfinate.

Complex **7** then undergoes extrusion of SO_2 to give complex **8** (δ_P = 18.50 ppm) having a molecular formula of (4-Me-C_6H_4)Pd$(PCy_3)_2$(OAc). The corresponding phenyl complex was reported and characterized by X-ray crystallography by Eastgate and co-workers.[21a] Above 100 °C, complex **8** is then likely to undergo a second acetate/aryl sulfinate exchange to form a palladium sulfinate complex $(Ar')Pd(PCy_3)_2(O_2SAr')$, followed by extrusion of SO_2 and reductive elimination to generate a palladium zero intermediate and 4,4′-dimethylbiphenyl, the homocoupling product. Neither of these two intermediates were observed by NMR spectroscopy as the rate of extrusion of SO_2 from such palladium sulfinate complexes (sections 2.2.3.2 and 2.5), and of oxidative addition (section 2.2.2), are expected to be fast at such temperatures. Instead, the oxidative addition complex (4−F-C_6H_4)Pd$(PCy_3)_2$(Br) **9** (δ_P = 20.08 ppm) was observed. Complex **8** can also undergo an acetate/bromide exchange giving complex **8b** (δ_P = 19.79 ppm), which can then undergo similar transformations leading to the formation of palladium zero and homocoupling product. Phosphine oxidation products were detected in trace amounts only, which is consistent with the observation that Pd$(PCy_3)_2(OAc)_2$ **6** is not easily reduced to palladium(0) via phosphine oxidation in the absence of hydroxide bases.[21a]

When the cross-coupling was performed using 5−18 mol % of $Pd(OAc)_2$ and PCy_3 in a 1:2 ratio, respectively, a linear correlation was observed between the amount of homocoupling product (4,4′-dimethylbiphenyl) formed and the amount of $Pd(OAc)_2$ introduced (see the SI), which supports the proposed reduction pathway of the precatalyst.

When sodium pyridine-2-sulfinate **1** was employed as the nucleophilic coupling partner, a different palladium complex **10** was isolated (Figures 2a and 2c). This complex also displays a square planar geometry around the Pd center, with a pyridine residue lying trans to the phosphine instead of a second phosphine ligand as in **7**. Two 2-pyridyl sulfinate groups are present in **10**. One chelates the palladium in a $\kappa^2_{N,O}$-mode, affording a five-membered metallocycle. This mode of ligand binding has precedence in copper 2-pyridyl sulfinate complexes.[31] The second 2-pyridyl sulfinate coordinates the palladium by the sulfur, trans to the oxygen binding. The Pd−S bond length in **10** (2.2307(5) Å) is notably shorter than that in **7**, possibly reflecting the decreased steric congestion in the former.

2.2.2. Oxidative Addition Complex. Once the active Pd(0) species have been generated, the next step of the presumed mechanism is the oxidative addition of the carbon−halide bond to the Pd(0) intermediate. Oxidative addition of bromobenzene to $Pd(PCy_3)_2$ has been investigated by Baird

https://dx.doi.org/10.1021/jacs.9b13260
J. Am. Chem. Soc. 2020, 142, 3564−3576

and co-workers[32] and Hartwig and co-workers.[33] Although these studies were conducted in nonpolar solvents and at room temperature, both concluded that the oxidative addition was an irreversible process that involved the aryl bromide substrate and the two-coordinate palladium zero complex $Pd(PCy_3)_2$, leading to the formation of compounds with the generic formula $(Ar)Pd(PCy_3)_2(Br)$. The oxidative addition complex $(4\text{-}F\text{-}C_6H_4)Pd(PCy_3)_2(Br)$ **9** was synthesized independently, according to literature procedures,[34] and proved to be a competent catalyst for our sulfinate coupling reactions, giving similar reaction rate and yield, compared to the mixture of $Pd(OAc)_2$ and PCy_3 (see the SI).

2.2.3. Palladium Sulfinate Complexes. For cross-coupling processes in general, the transmetalation step, which involves the oxidative addition complex and the nucleophilic coupling partner, differs for each nucleophile, leading to a wide variety of mechanisms and palladium intermediates. Such post-transmetalation complexes have been characterized for several nucleophiles, including alcohols,[35] amines,[36] thiols,[37] and carboxylic acids.[38] However, despite having been reported as efficient coupling partners, to the best of our knowledge, there is no report of a post-transmetalation intermediate with a nucleophilic sulfinate. A dimeric palladium sulfinate complex with bridging Cl^- anions has recently been reported by Shavnya and co-workers;[39] however, it is not relevant to an oxidative addition/transmetalation sequence. In the studied cross-coupling, putative palladium sulfinate intermediates would arise from the displacement of the Br atom from oxidative addition complex **9** by a metal sulfinate salt, as described in Scheme 3.

Scheme 3. Putative Formation of the Palladium Sulfinate Complexes

$$(Ar)Pd(PCy_3)_n(Br) + MO_2SAr' \rightarrow (Ar)Pd(PCy_3)_n(O_2SAr') + M\text{-}Br$$

Unlike carboxylate salts, metal sulfinate complexes can have different coordination modes, binding through sulfur, oxygen, or both.[40] In the previous section, we have described two types of palladium sulfinate complexes relevant to the reduction of Pd(II) to Pd(0). In the following section, we describe the first synthesis and characterization of post-transmetalation aryl palladium sulfinate complexes.

2.2.3.1. Synthesis and Characterization. We first attempted to form the transmetalation complexes by heating the oxidative addition complex **9** at moderate to elevated temperatures (50−120 °C) in the presence of the carbocyclic sulfinate salt **4**. However, formation of biaryl **5** and/or decomposition were observed. In the presence of silver nitrate, the oxidative addition complex was entirely consumed at room temperature, and we isolated the dimeric palladium sulfinate complex **11** (Figures 3a and 3b). When the pyridine-2-sulfinate substrate **1** was subjected to the same reaction conditions, the monomeric palladium sulfinate complex **12** was obtained (Figures 3a and 3c). The geometry about the palladium center in **12** closely resembles that present in **10**. The Pd−O bond length in complex **12** (2.132(2) Å) is elongated, relative to that in complex **10** (2.0975(13) Å), reflecting the greater trans influence of the aryl ligand. A similar square planar geometry about the palladium is observed in complex **11**; however, the absence of a pyridyl substituent on the sulfinate results in the vacant site being occupied by the S atom of a neighboring

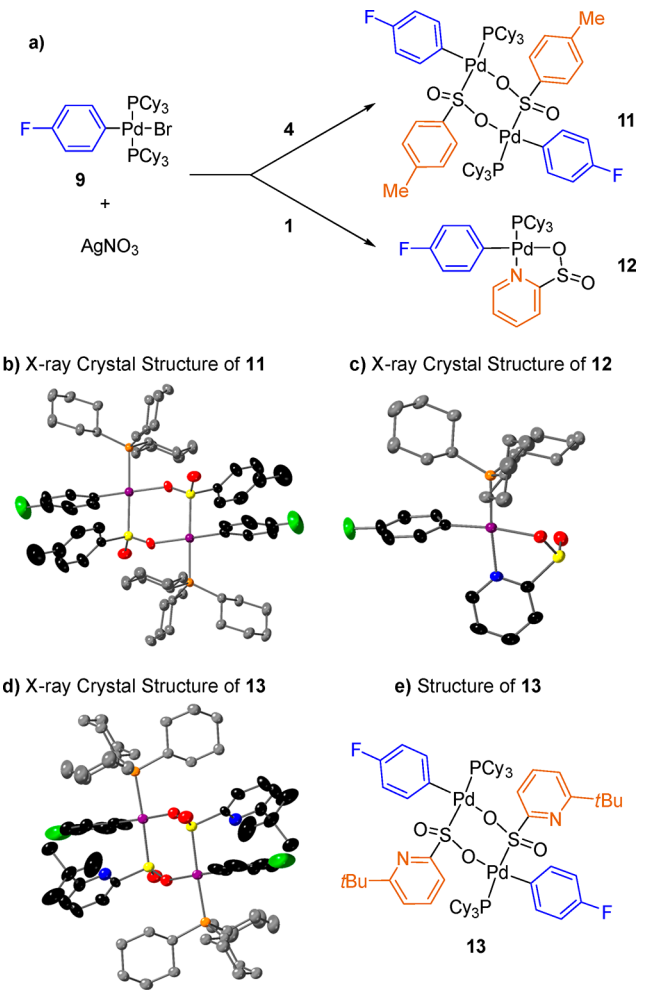

Figure 3. (a) Synthesis of the palladium sulfinate complexes **11** and **12**. X-ray crystal structures (50% displacement ellipsoids) of (b) **11**, (c) **12**, and (d) **13**. (e) Structure of **13**. All H atoms have been omitted for the sake of clarity.

sulfinate, affording a dimeric structure. The structure is similar to that of $[(PMe_3)Pd(CH_2CMe_2C_6H_4SO_2)]_2$, which likewise features a trans-phosphorus−sulfur configuration.[41] The bond lengths and angles observed in **11** also resemble those in $[(PMe_3)Pd(CH_2CMe_2C_6H_4SO_2)]_2$.

The diffusion coefficients obtained by DOSY NMR spectroscopy predicted masses for complexes **11** and **12** in a 2:1 ratio, indicating that the former maintains its dimeric structure in solution. The degree of aggregation in these complexes is also maintained when either an electron-donating or electron-withdrawing substituent is introduced at the position para to the sulfinate group (see the SI).

A notable exception is when steric bulk, in the form of a *tert*-butyl group, is placed at the 6-position of the pyridine. This prevents the $\kappa^2_{N,O}$-binding mode of the pyridine sulfinate, thereby affording a dimeric solid-state structure **13** which resembles that of the 4-methylbenzenesulfinate substituted complex, **11** (Figure 3d). X-ray-suitable crystals could be obtained from CH_2Cl_2/hexane recrystallization of crude reaction mixtures; however, attempts to obtain analytically pure samples for this compound were unsuccessful.

2.2.3.2. Reactivity. When the dimeric complex **11** was subjected to 1.1 equiv of PCy_3, its resonance peak at $\delta_P = 27.77$ ppm disappeared and was replaced by a doublet at $\delta_P = 21.95$

https://dx.doi.org/10.1021/jacs.9b13260
J. Am. Chem. Soc. 2020, 142, 3564−3576

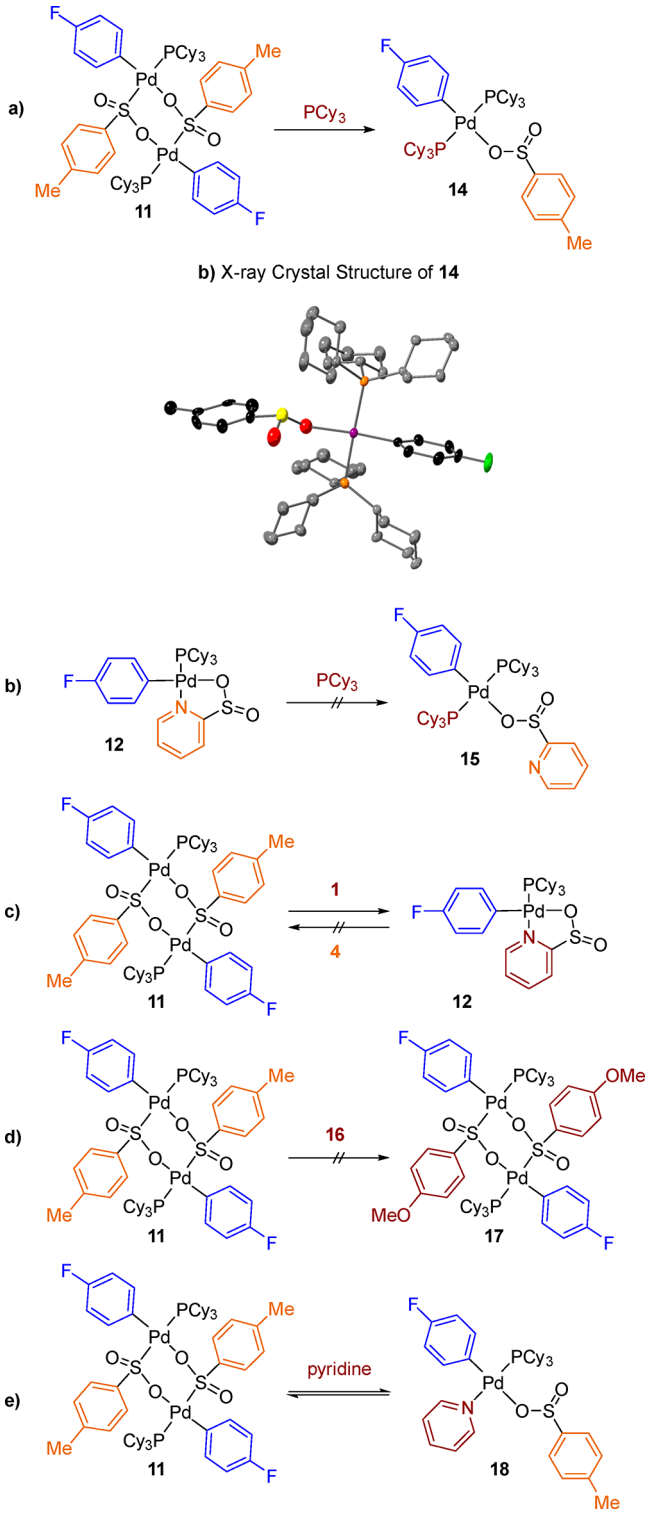

Figure 4. Reactivity of the palladium sulfinate complexes **11** and **12** at room temperature in 1,4-dioxane/benzene-d_6 5:1. X-ray crystal structure (50% displacement ellipsoids) of **14**. All H atoms have been omitted for the sake of clarity. **16** = 4-MeO-C_6H_4–SO_2Na.

ppm, J_{P-F} = 3.0 Hz. This new signal is very similar to the resonance peak observed for the oxidative addition complex **9** (δ_P = 20.20, J_{P-F} = 3.0 Hz). Although the conversion was quantitative according to the $^{19}F\{^1H\}$ NMR spectrum, the new complex was only isolated in 57% yield. Crystals suitable for XRD were obtained, and the identity of complex **14** was confirmed as a square planar palladium complex bearing two phosphine ligands (Figure 4a). The solid-state structure of **14** closely resembles that of **7**; however, unlike in the latter, the sulfinate binds to palladium via the O atom, rather than a S atom. This is consistent with a nucleophilic displacement of the S atom from dimeric complex **11**. While the addition of a phosphine to the dimeric complex **11** occurs at room temperature, the pyridine sulfinate containing palladacycle **12** was unreactive toward PCy_3, and compound **15** was not observed, suggesting that the Pd–N bond in **12** is much stronger than the Pd–S bond in dimeric complex **11** (Figure 4b). Accordingly, formation of complex **12** was observed at room temperature upon combining dimeric complex **11** and sodium pyridine-2-sulfinate **1**, whereas the reverse reaction was not observed under the same conditions (Figure 4c). Exchange between two carbocyclic sulfinates was not observed at room temperature either, as dimeric complex **17** was not observed when the more nucleophilic 4-methoxybenzene-sulfinate salt **16** was combined with dimeric complex **11** (Figure 4d). However, the Pd–S bond of **11** could be cleaved upon addition of excess pyridine (Figure 4e). A new complex was observed by NMR spectroscopy and assigned as complex **18**, but its isolation was not possible, since **11** was recovered after workup.

When 4-methylbenzenesulfinate palladium complex **11** was heated at 90 °C in toluene-d_8, it was fully consumed within 20 min with concomitant formation of biaryl **5** (Figure 5, gray diamonds). Complex **14** (generated in situ from **11** and PCy_3) reacted at a slower rate, but gave 84% conversion within 45 min (Figure 5, yellow triangles). Increasing the concentration of PCy_3 resulted in a significant decrease of the rate of SO_2 extrusion at 90 °C, suggesting that ligand dissociation is necessary prior to desulfination (see the SI). The pyridine-2-sulfinate palladacycle **12** in which the sulfinate chelates the palladium in a $\kappa^2_{N,O}$-mode only gave 11% conversion after 45

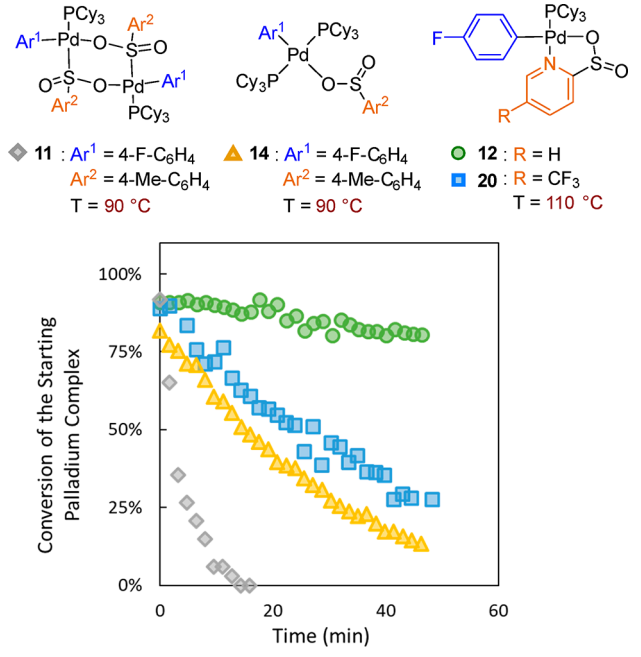

Figure 5. Reactivity of the palladium sulfinate complexes upon heating. Reactions were performed in toluene-d_8 in a Young's NMR tube. Complex **14** was generated in situ from complex **11** and tricyclohexylphosphine.

https://dx.doi.org/10.1021/jacs.9b13260
J. Am. Chem. Soc. 2020, 142, 3564–3576

min at 110 °C (Figure 5, green circles). Weakening the Pd−N bond by adding an electron-withdrawing group on the pyridyl ring, as in complex **20**, increased the rate of extrusion of SO_2 in toluene-d_8, as a 70% conversion was obtained after 45 min at 110 °C (Figure 5, blue squares). The relative rates of consumption of the complexes shown in Figure 5 have been shown to correspond to the rates of formation of the cross-coupling products (see the SI).

Overall, these experiments show that the S−Pd bond present in dimer **11** can readily be displaced by nitrogen- or phosphorus-based nucleophiles. The formation of five-membered-ring palladacycles with the pyridine-2-sulfinate substrates renders the derived palladium sulfinate complexes more thermodynamically stable, and dramatically slows the extrusion of SO_2. In addition, we have shown that complexes **11**, **12**, and **14** are competent catalysts for their respective coupling reactions (see the SI).

2.3. Identification of the Resting-State Intermediates.

To identify the resting-state intermediates of the catalytic reactions, the desulfinative cross coupling was monitored by $^{31}P\{^1H\}$ NMR and $^{19}F\{^1H\}$ NMR spectroscopy. The reactions were performed in a Young's NMR tube with a higher loading of $Pd(OAc)_2$ and PCy_3 (15 mol % and 30 mol %, respectively). The observed resonance peaks were compared to the signals of reference samples acquired in a 5:1 mixture of 1,4-dioxane/benzene-d_6. Because of poor stirring of the heterogeneous mixture in an NMR tube, the reaction kinetics were found to be very slow. After 14 h at 150 °C, at which point biaryl **5** was formed in 40% yield (~2.7 turnovers), the resonance peak of the oxidative addition complex **9** (δ_F = −124.26 ppm) was the only other signal observed on the $^{19}F\{^1H\}$ spectrum along with starting material, internal standard, and product (Figure 6a). The corresponding characteristic doublet at δ_P = 20.08 ppm was also observed in the $^{31}P\{^1H\}$ spectrum, along with free PCy_3 (δ_P = 9.24 ppm), phosphine oxide (δ_P = 45.65 ppm) and compound **8** (δ_P = 19.80 ppm) (Figure 6c). Therefore, the oxidative addition complex **9** is likely to be the resting-state intermediate when using carbocyclic sulfinate **4**. The same experiment was performed with the pyridine-2-sulfinate substrate **1**. After 14 h of reaction at 150 °C, the conversion to product **3** was lower than for the carbocyclic substrate (20%, ~1.3 turnovers). The oxidative addition product **9** was observed in a 1:1 ratio with palladium sulfinate complex **12** (Figure 6b). The corresponding phosphorus resonance peaks (δ_P = 38.03 and δ_P = 20.08), along with free PCy_3 oxidation products, were also observed (Figure 6d).

In section 2.2.3.2, we have assessed the reactivity of the palladium sulfinate complexes and demonstrated that weakening of the N−Pd bond facilitates the extrusion of SO_2 from the palladium pyridine-2-sulfinate complexes. When sodium 5-(trifluoromethyl)pyridine-2-sulfinate **19** was subjected to the cross-coupling conditions in a Young's NMR tube, the corresponding palladium sulfinate complex **20** could not be detected by $^{19}F\{^1H\}$ or $^{31}P\{^1H\}$ NMR, and the oxidative addition complex **9** was the only observable complex by $^{19}F\{^1H\}$ NMR spectrum (see the SI). Similarly, sodium pyridine-4-sulfinate **21**, which does not have the appropriate substitution pattern to form a stabilizing N−Pd interaction, only exhibited the resonance of the oxidative addition complex **9** (see the SI). Unidentified minor resonances were detected at δ_P = 19.81 ppm and δ_P = 20.17 ppm, together with free ligand and minor phosphine oxide peaks. Finally, the oxidative addition complex **9** was once again the only resonance observed in the $^{19}F\{^1H\}$ spectrum when the bulky lithium 6-(*tert*-butyl)pyridine-2-sulfinate **22** was used. This is consistent with the observation of the dimeric crystal structure of the 6-*tert*-butylsulfinate containing palladium complex **13**, as the formation of a $\kappa^2_{N,O}$-chelate is hindered by the *tert*-butyl group, showing that the bulky pyridine sulfinate salt behaves in a manner similar to that of a carbocyclic substrate.

Since the concentration, stirring, and therefore kinetics in an NMR tube are not accurately representative of the actual reaction conditions, the two cross-coupling reactions involving sodium pyridine-2-sulfinate **1** and sodium 4-methylbenzenesulfinate **4** were also performed in microwave tubes at a relevant scale. The tubes were heated for 2 h at 150 °C, then 500 μL of the reaction mixture were transferred to an NMR tube containing 100 μL of benzene-d_6. The observed resonance peaks were in agreement with the reactions performed in the Young's NMR tubes. One difference was observed for the cross-coupling of pyridine-2-sulfinate salt **1** for which the ratio between the oxidative addition complex **9** and the pyridine sulfinate complex **12** was found to be 1:3.8 instead of 1:1 (see the SI). The use of an appropriate reaction vial equipped with a stirrer bar instead of Young's NMR tube must ease the transmetalation step, which involves the poorly soluble sulfinate salt, while the rate of extrusion of SO_2 remains unaffected and difficult, because of the strong $\kappa^2_{N,O}$-chelation mode. As a consequence, the resting-state intermediate is shifted from the oxidative addition complex **9** to the pyridine-2-sulfinate containing palladium complex **12**.

Overall, these experiments show that the resting state of the catalyst is highly dependent on the nature of the sulfinate coupling partner and is more likely to be the oxidative addition

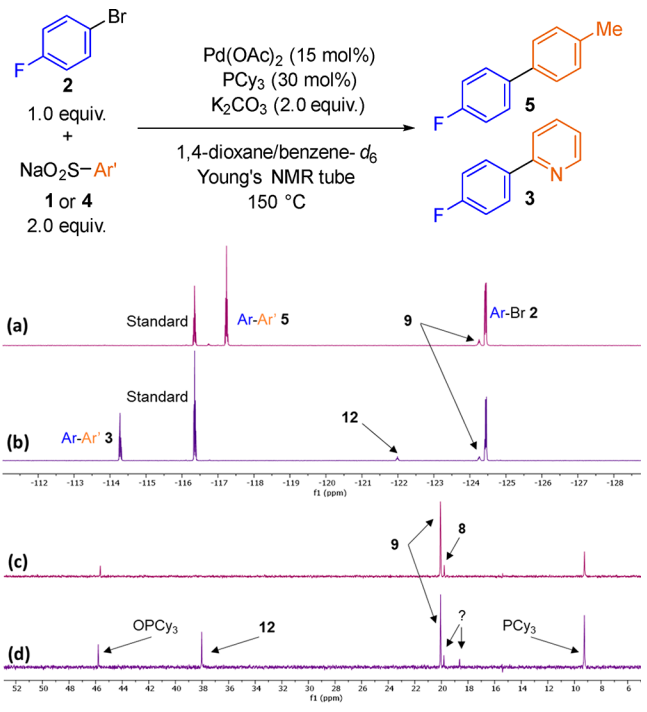

Figure 6. Cross-coupling reactions performed in a Young's NMR tube. (a) $^{19}F\{^1H\}$ NMR spectrum of the reaction mixture involving sulfinate **4**. (b) $^{19}F\{^1H\}$ NMR spectrum of the reaction mixture involving sulfinate **1**. (c) $^{31}P\{^1H\}$ NMR spectrum of the reaction mixture involving sulfinate **4**. (d) $^{31}P\{^1H\}$ NMR spectrum of the reaction mixture involving sulfinate **1**.

https://dx.doi.org/10.1021/jacs.9b13260
J. Am. Chem. Soc. 2020, 142, 3564−3576

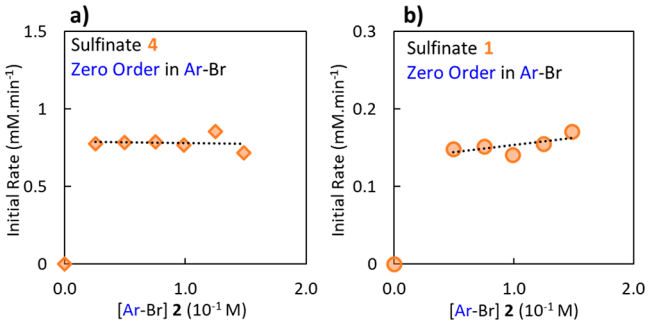

Figure 7. Initial rate plots for cross coupling between aryl bromide **2** and (a) sodium 4-methylbenzenesulfinate **4** (orange diamonds) and (b) sodium pyridine-2-sulfinate **1** (orange circles).

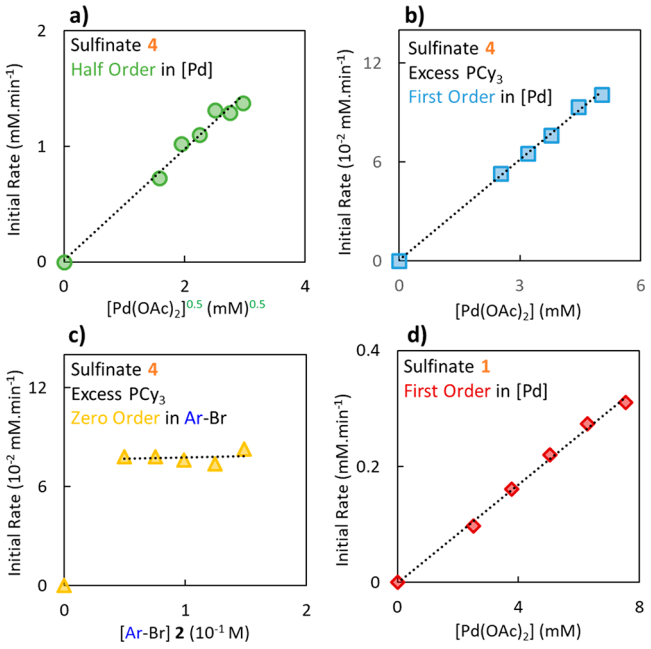

Figure 8. Initial rate plots for cross coupling between aryl bromide **2** and (a) 4-methylbenzenesulfinate **4** (green circles), (b) 4-methylbenzenesulfinate **4** using an excess of PCy_3 (blue squares), (c) 4-methylbenzenesulfinate **4** using an excess of PCy_3 (gold triangles), and (d) pyridine-2-sulfinate **1** (red diamonds).

complex **9** for carbocyclic sulfinates or for pyridine-sulfinate substrates that cannot form strong N−Pd bonds, due to geometrical, steric, or electronic reasons. A strong $\kappa^2_{N,O}$-chelation as observed for the unsubstituted pyridine-2-sulfinate group in the palladium sulfinate complex **12** was observed to cause a change in the resting-state intermediate.

2.4. Initial Rate Studies. Productive catalytic reactions are performed at 150 °C in 1,4-dioxane (boiling point (bp) = 101 °C) and involve partially soluble reagents such as the sulfinate salts and potassium carbonate, leading to suspensions rather than homogeneous solutions. Therefore, the reactions could not be accurately monitored by NMR spectroscopy and were monitored using HPLC analysis of aliquots taken from the reaction mixture via syringe, and the partial orders were obtained using the initial rates of the reactions.

2.4.1. Order in Aryl Bromide. The reactions of 4-methylbenzenesulfinate **4** and pyridine-2-sulfinate **1** were performed with different concentrations of aryl bromide **2** (0.025−0.15 mM).

The initial rates were not affected by the concentration of the electrophilic coupling partner (Figures 7a and 7b). This zero-order behavior suggests that oxidative addition of the C−Br bond into the Pd(0) species is not the turnover limiting step under the reaction conditions. This observation is in agreement with the observed resting-state intermediates in section 2.3.

2.4.2. Order in Sulfinate Salt and K_2CO_3. It was observed that 0.010−0.10 M solutions of sodium 4-methylbenzenesulfinate **4** or sodium pyridine-2-sulfinate **1** are heterogeneous at 150 °C. Therefore, the partial orders in sulfinate coupling partner were not measured. Similarly, the order in potassium carbonate was not obtained.

2.4.3. Order in Catalyst. To get the partial order in catalyst, the initial rate of the reaction was measured for different concentrations of $Pd(OAc)_2$ and PCy_3, keeping the ligand to palladium ratio fixed at two. The rate of the reaction involving 4-methylbenzenesulfinate sodium salt **4** was observed to be approximately proportional to the square root of the total concentration of palladium introduced, as palladium acetate: rate $\propto [Pd(OAc)_2]^{0.5}$ (Figure 8a). Half order in catalyst can generally be rationalized by an equilibrium between a catalytically active complex and an off-cycle species. This can be caused by dimerization of the active catalyst to form an inactive dimer.[42] Half-order dependence of the catalyst can also arise from ligand dissociation.[43] When the concentration of $Pd(OAc)_2$ was varied while the phosphine ligand was in excess, such as $[Pd(OAc)_2]/[PCy_3] < 0.10$, the half-order dependence on the concentration of palladium acetate was no longer observed. Instead, the rate was observed to be directly proportional to the concentration of $Pd(OAc)_2$: rate $\propto [Pd(OAc)_2]$ (Figure 8b).

Therefore, the half-order dependence observed can be taken into account by a fast equilibrium between the catalytically inactive oxidative addition intermediate $(Ar)Pd(PCy_3)_2(Br)$ and the reactive intermediate $(Ar)Pd(PCy_3)(Br)$ generated after the loss of a phosphine ligand (Scheme 4). However, the rate of oxidative addition is known to decrease dramatically upon the addition of ligand, as the inactive tris-ligated $Pd^0(PCy_3)_3$ can be formed.[44] In order to verify that the switch between half-order and first-order is not due to a change of turnover-limiting step, the order in aryl bromide was determined for a Pd/L ratio <0.10 (Figure 8c). A zero-order case was obtained under these conditions, showing that the oxidative addition is not rate-determining in the presence of excess ligand.

Scheme 4. Interpretation of the Initial Rates for the Carbocyclic Sulfinate 4

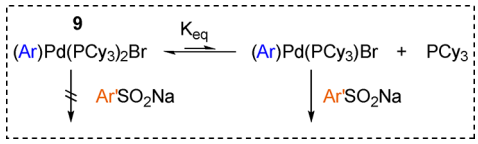

In order to assess the lability of PCy_3 under the reaction conditions, the analogous oxidative addition complex **23** was synthesized with the electronically and sterically similar triisopropylphosphine P*i*-Pr$_3$.[45] When the two oxidative addition complexes were heated at 75 °C in a 5:1 mixture of 1,4-dioxane/benzene-d_6, statistical scrambling was obtained within 2 h and the mixed complex **24** was observed (Scheme 5).

https://dx.doi.org/10.1021/jacs.9b13260
J. Am. Chem. Soc. 2020, 142, 3564−3576

Scheme 5. Lability of PCy_3 under the Reaction Conditions

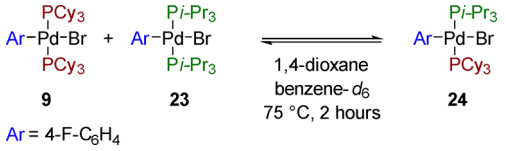

Therefore, PCy_3 is likely to be labile under the reaction conditions, which supports the phosphine dissociation/transmetalation sequence.

The rate of the reaction involving sodium pyridine-2-sulfinate **1** was directly proportional to the concentration of palladium acetate: rate ∝ $[Pd(OAc)_2]$ (Figure 8d). There is no longer a half-order dependence in $Pd(OAc)_2$ as observed for the carbocyclic sulfinate **4**. This is in agreement with the observation of different resting-state intermediates for reactions involving substrates **1** and **4**. For the former, the first order dependence in $Pd(OAc)_2$ is consistent with the catalyst resting state being palladium sulfinate complex **12** and the rate-determining step being the extrusion of SO_2. As a half-order dependency is not observed for pyridine-2-sulfinate **1**, this suggests that the transmetalation is irreversible under these reaction conditions.

2.5. Comparison of the Rates of Transmetalation and SO_2 Extrusion. Stoichiometric reactions involving the oxidative addition complex **9** or the palladium sulfinate complexes **11** and **12** were performed in order to qualitatively compare the rates of transmetalation and extrusion of SO_2. For the reaction involving the oxidative addition complex **9**, 2 equiv of the potassium sulfinate salts **25** or **26** were employed (Figure 9). The potassium salts were chosen for these stoichiometric studies, since evidence suggests that these are the salts formed in the catalytic reactions when K_2CO_3 is used as the base (section 2.6.2). When the dimeric complex **11** was heated at 150 °C with 1−4 equiv of PCy_3, with respect to the amount of palladium, full conversion to the corresponding biaryl **5** was obtained within 2 min (Figure 9a). Although we have demonstrated that added phosphine slows the rate of extrusion of SO_2 at 90 °C in toluene-d_6 (see the SI), these data show that the concentration of ligand does not affect the rate of extrusion of SO_2 from the in-situ-generated complex **14** at 150 °C. However, the rate of the transmetalation/SO_2 extrusion sequence was dramatically slowed upon the addition of PCy_3 (Figure 9b). An excess of phosphine is likely shifting the equilibrium between the transmetalation inactive (Ar)Pd(PCy$_3$)$_2$(Br) **9** and the transmetalation active (Ar)Pd(PCy$_3$)(Br) toward **9**, slowing the overall rate of product formation. These observations are consistent with a turnover-limiting transmetalation after the loss of ligand from oxidative addition complex **9**, as exposed in section 2.4.3.

For pyridine-2-sulfinate palladium complex **12**, the rate of extrusion of SO_2 was much slower than for carbocyclic complex **11** (Figure 9c). Indeed, independent of the concentration of ligand, at least 20 min were necessary to reach >90% conversion, compared to <2 min for the carbocyclic system. The concentration of ligand did not affect the rate of SO_2 extrusion at 150 °C. Compared to the reaction with the carbocyclic sulfinate in Figure 9b, ligand concentration had little impact on the observed rate of product formation for the transmetalation/extrusion of SO_2 sequence with potassium pyridine-2-sulfinate **26** (Figure 9d). This is consistent with the rate-determining step of the transmetalation/SO_2 extrusion sequence being cleavage of the Pd−N bond of the palladacycle **12**, which should be independent of ligand concentration.

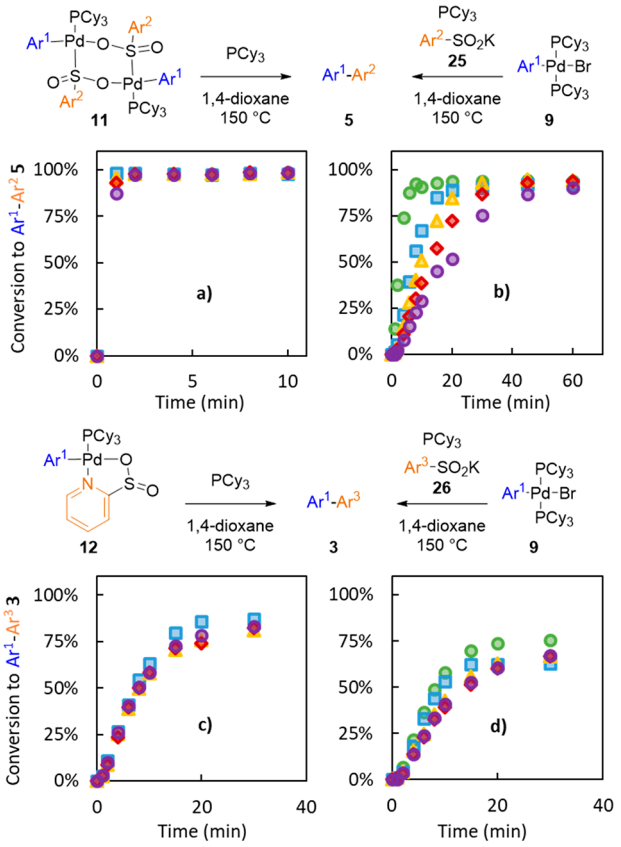

Figure 9. Comparison of the rates of the SO_2 extrusion and of the sequence of transmetalation/SO_2 extrusion for both carbocyclic sulfinate **4** and pyridine-2-sulfinate **1**. Pd_{total} (1.0 equiv), PCy_3 (0−4.0 equiv), Ar^2SO_2K (2.0 equiv), Ar^3SO_2K (2.0 equiv). Ar^1 = 4−F-C_6H_4; Ar^2 = 4-Me-C_6H_4; Ar^3 = 2-pyridyl. [Legend: green circles, 0 equiv PCy_3; blue squares, 1.0 equiv PCy_3; gold triangles, 2.0 equiv PCy_3; red diamonds, 3.0 equiv PCy_3; and purple circles, 4.0 equiv. PCy_3.]

This set of stoichiometric experiments is in good agreement with the partial orders in catalyst obtained using substoichiometric amounts of $Pd(OAc)_2$ in section 2.4.

2.6. Role of K_2CO_3. Unlike for the coupling of aryl halides with nucleophiles such as amines, alcohols, or thiols, there are no acidic protons to be removed in the coupling of sulfinate salts. Yet, a carbonate base, and, more specifically, potassium or cesium carbonate, is a crucial additive for the reaction. In the following section, we investigated the role of the carbonate base and of its countercation.

2.6.1. Role of the Carbonate. One molecule of sulfur dioxide is extruded every time a molecule of the biaryl product is generated. Therefore, since 5 mol % of $Pd(OAc)_2$ is used, a 20:1 ratio between the gaseous byproduct and the catalyst is reached at the end of the reaction. Since SO_2 gas and SO_2 surrogates have been utilized in many palladium-catalyzed C−S bond-forming reactions,[20b,46] the SO_2 generated in the present reactions is likely to coordinate to the palladium center, potentially disrupting catalysis.

Carbonate bases are reported to be efficient traps for SO_2 gas in the waste stream from combustion in several industrial processes.[47] Given this, we hypothesized that a carbonate base was necessary to trap the liberated SO_2 in the reaction under

https://dx.doi.org/10.1021/jacs.9b13260
J. Am. Chem. Soc. 2020, 142, 3564−3576

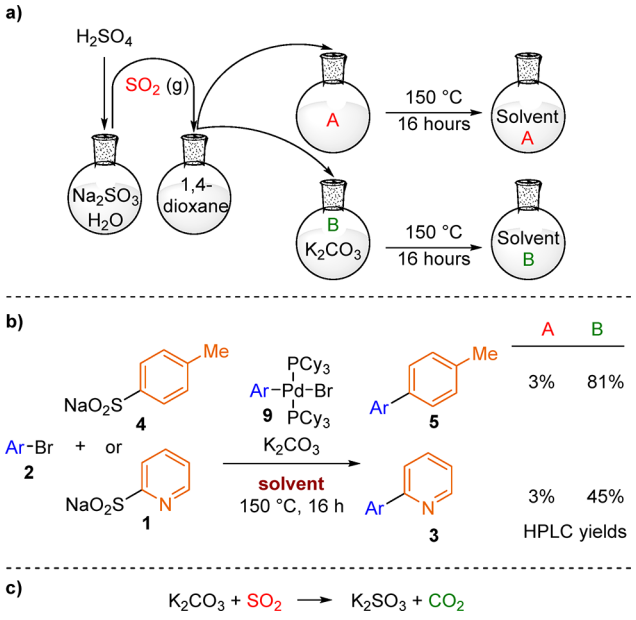

Figure 10. Influence of SO_2 and K_2CO_3 on the reaction: (a) generation of gaseous SO_2, solvents A and B; (b) reaction outcome; and (c) rationalization of the role of K_2CO_3.

study, preserving the catalyst and allowing reasonable turnover to be achieved. In order to test this, 0.05 M solutions of SO_2 gas in 1,4-dioxane were prepared and divided into an empty flask (A) or a flask containing K_2CO_3 (B). These flasks were then heated at 150 °C for 16 h, which are the standard reaction time and temperature employed in productive catalytic cross-coupling reactions (Figure 10a). The obtained solvents A and B were then used for reactions between aryl bromide **2** and carbocyclic and pyridine sulfinates **1** and **4**, catalyzed by the oxidative addition product **9**. For both substrates, 3% product

Scheme 6. Toward a Lower Temperature Cross-Coupling[d]

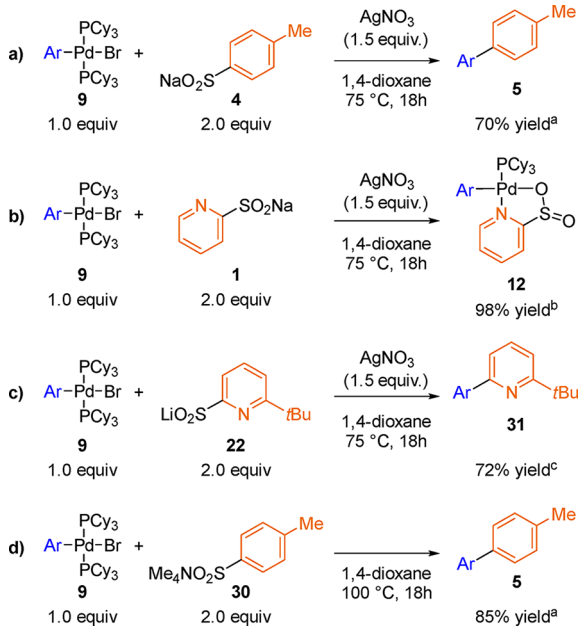

[a]HPLC yield against 1,3,5-trimethoxybenzene. [b]^{19}F NMR yield based on starting material consumption. [c]^{19}F NMR yield against 1-fluoronaphtalene. [d]Ar = 4-F-C_6H_4.

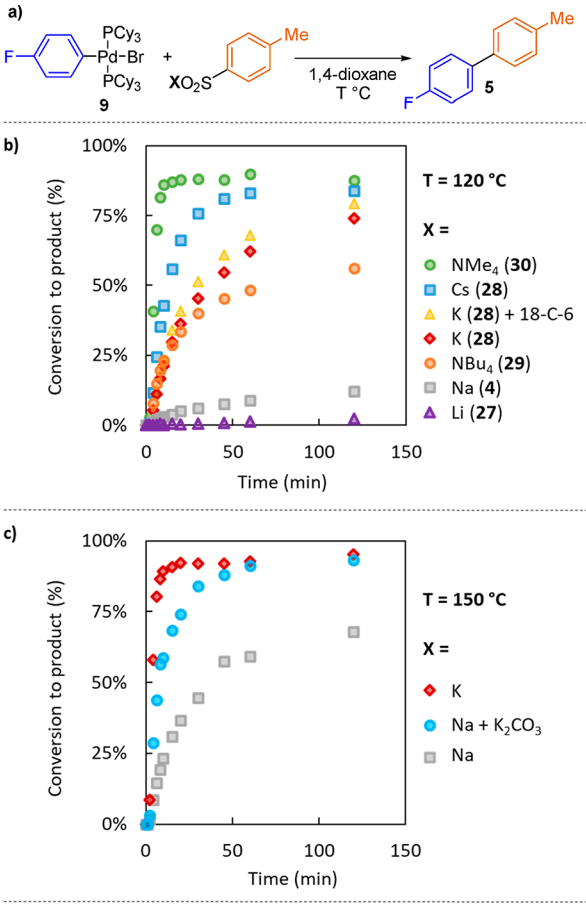

Figure 11. Influence of the cation on the rate of the transmetalation step.

(less than one turnover) was obtained when using solvent A. Conversely, solvent B, which contained K_2CO_3, provided 81% and 45% yields of products **5** and **3**, respectively (Figure 10b). These experiments show the importance of the carbonate base to sequester SO_2. Based on literature reports,[47,48] we conclude that sulfite anions are generated together with carbon dioxide, as shown in Figure 10c.

2.6.2. Role of the Cation. We demonstrated in sections 2.4. and 2.5 that the reaction involving pyridine-2-sulfinate sodium salt **1** is limited by the rate of SO_2 extrusion, which does not involve the original sulfinate cation. Therefore, the role of the cation was studied for the reaction involving the carbocyclic sulfinate **4**, in which the cation is likely to be involved between the resting-state intermediate and the turnover-limiting step. We also showed in section 2.5 that the rate of extrusion of SO_2 is extremely fast, compared to the rate of transmetalation for the carbocyclic substrate **4**. Therefore, in the following section, we have considered that the rate of product formation in the reaction between the oxidative addition complex and a sulfinate salt is representative of the rate of the transmetalation step. The reactions were performed at 120 °C using 2 equiv of sulfinate to 1 equiv of oxidative addition product **9** (Figure 11a).

Lithium sulfinate **27** showed almost no reactivity (2% product formation in 2 h). Similarly, sodium sulfinate **4** provided 12% product within 2 h, whereas potassium sulfinate **25** reached 74% conversion to product (Figure 11b). Moving further down in the alkaline metals group, cesium sulfinate **28**

https://dx.doi.org/10.1021/jacs.9b13260
J. Am. Chem. Soc. 2020, 142, 3564−3576

Scheme 7. Overall Mechanism

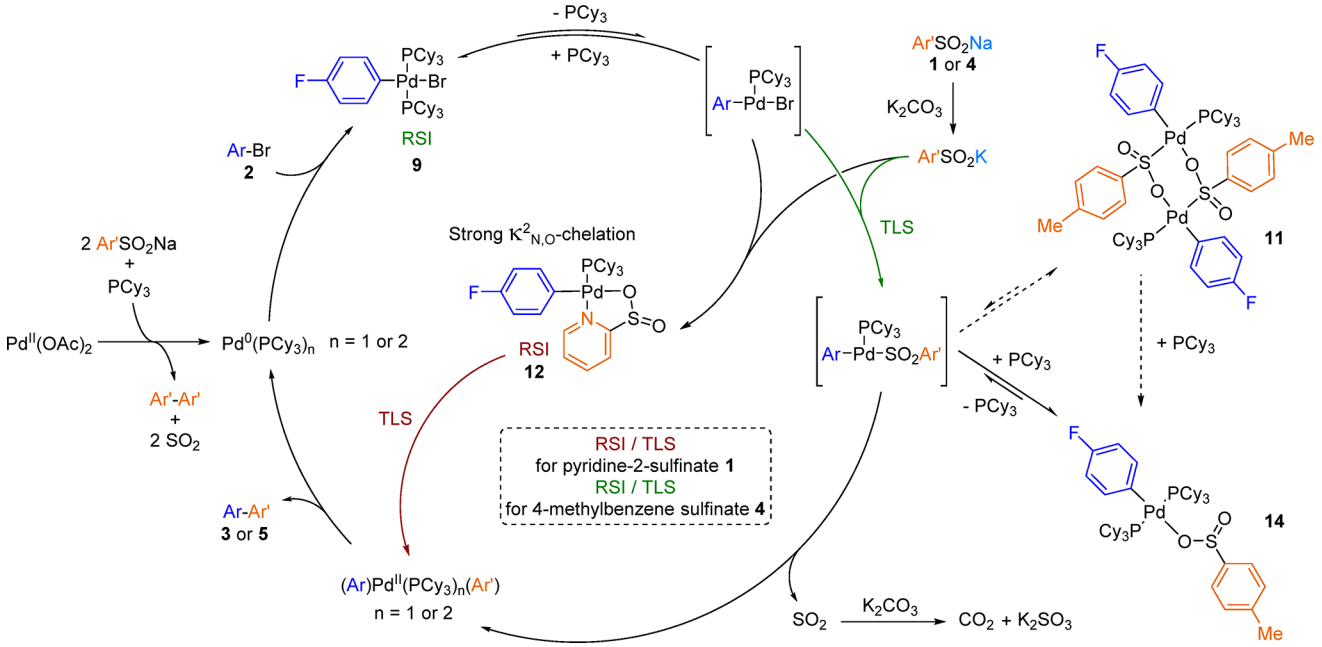

increased the rate significantly, with 84% product formation in the same time. Tetrabutylammonium sulfinate **29** had a similar initial rate, compared to the potassium sulfinate **20**. However, the conversion did not rise above 60%, even after 5 h. This could be caused by Hofman-type elimination of the ammonium salt, leading to substrate decomposition. The use of 18-crown-6 only slightly increased the rate of anion exchange with 79% yield after 2 h. However, a dramatic increase in rate was observed with tetramethylammonium sulfinate **30**, which led to 86% yield within the first 10 min. The low performance of the tetrabutylammonium sulfinate salt, compared to the potassium, or cesium sulfinates suggests that solubility of the sulfinate salt is not correlated to the rate of the transmetalation step. Indeed, the tetrabutylammonium sulfinate is entirely soluble in 1,4-dioxane at 120 °C, while the alkali sulfinates are not. Tetramethylammonium salts have been used as silver surrogates to abstract halide atoms,[49] which might explain the excellent reactivity of sulfinate **30** in the transmetalation step. When sodium sulfinate **4** was employed in a 1:1 ratio with K_2CO_3 at 150 °C, the transmetalation occurred almost as quickly as the transmetalation involving potassium sulfinate **25** (Figure 11c). This suggests that the role of K_2CO_3, in addition to trapping liberated SO_2, is to take part in a cation metathesis with the sodium sulfinate salt, thus facilitating transmetalation.

2.7. Toward Lower Temperatures. In section 2.2.3.1, the use of the silver salt $AgNO_3$ allowed the synthesis of a variety of palladium sulfinate complexes at room temperature, starting from the oxidative addition complex **9**. In other words, this additive allowed the transmetalation step to occur 125 °C below the temperatures needed in the catalytic system, presumably because of the high affinity between Ag and Br atoms.[50] To confirm the viability of this additive based strategy for lowering the reaction temperature, stoichiometric reactions were performed between the oxidative addition complex **9** and carbocyclic and pyridyl sodium sulfinates **4** and **1** in the presence of $AgNO_3$. Cross-coupling product **5** was obtained in 70% yield for the carbocyclic sulfinate, showing the potential of silver additives to promote reactivity for these types of substrates (Scheme 6a). However, for the heterocyclic sulfinate **1**, only the corresponding palladium sulfinate complex **12** was obtained (Scheme 6b).

This suggests that an additive-based strategy that accelerates transmetalation will not be sufficient to achieve a lower temperature cross-coupling for substrates able to strongly chelate the palladium in a $\kappa^2_{N,O}$-fashion. For these systems, in addition to the transmetalation, there will be an additional challenge in disrupting the stabilizing chelation to the Pd center. This is consistent with the earlier results and was confirmed by the reaction shown in Scheme 6c, in which the sterically hindered 6-*tert*-butylpyridine-2-sulfinate salt **22** underwent a lower temperature cross coupling and delivered biaryl **31** in 72% yield. However, the use of silver salts was noncompatible with the catalytic reaction, presumably due to their ability to also act as oxidants.[51] The tetramethylammonium alternative proved to be promising, providing the cross-coupling product **5** in 85% yield in the stoichiometric reaction between the oxidative addition complex **9** and the tetramethylammonium sulfinate **30** at 100 °C (Scheme 6d). We are currently investigating the use of such additives in the catalytic reaction, as well as alternative strategies to achieve lower temperature cross-couplings with carbocyclic and heterocyclic substrates.

3. CONCLUSION

The mechanism of the palladium-catalyzed desulfinative cross-coupling of aryl halides and sulfinate salts was investigated. The in situ reduction of the Pd(II) source to form the active Pd(0) species was shown to be mediated by the homocoupling of two sulfinate substrates. Novel palladium sulfinate complexes were independently synthesized, characterized, and proven to be competent intermediates in the catalytic reaction. The resting-state catalyst and the rate-determining step were identified. Their identity was heavily dependent on the nature of the sulfinate coupling partner, more specifically on the ability of the sulfinate to strongly chelate the palladium

https://dx.doi.org/10.1021/jacs.9b13260
J. Am. Chem. Soc. 2020, 142, 3564−3576

in a $\kappa^2_{N,O}$-mode. The kinetic data also suggest that both transmetalation and extrusion of SO_2 most likely occurs after dissociation of a phosphine ligand in order to free a coordination site on palladium. Finally, we showed that the base has a dual role: the carbonate traps the generated sulfur dioxide and permits catalyst turnover, while the potassium countercation undergoes a cation metathesis with the sulfinate salt to allow a faster transmetalation step (Scheme 7).

In summary, isolation of novel palladium sulfinate complexes and kinetic analysis has allowed us to identify the key challenges to reduce the temperature of these reactions. Efforts toward reactions that proceed using milder conditions are currently underway.

■ ASSOCIATED CONTENT

Supporting Information

The Supporting Information is available free of charge at https://pubs.acs.org/doi/10.1021/jacs.9b13260.

Crystallographic data (CIF)

Experimental procedures and supporting characterization data and spectra (PDF)

■ AUTHOR INFORMATION

Corresponding Author

Michael C. Willis − *Department of Chemistry, Chemistry Research Laboratories, University of Oxford, Oxford OX1 4TA, United Kingdom;* orcid.org/0000-0002-0636-6471; Email: michael.willis@chem.ox.ac.uk

Authors

Antoine de Gombert − *Department of Chemistry, Chemistry Research Laboratories, University of Oxford, Oxford OX1 4TA, United Kingdom*

Alasdair I. McKay − *Department of Chemistry, Chemistry Research Laboratories, University of Oxford, Oxford OX1 4TA, United Kingdom; School of Chemistry, University of Melbourne, Parkville, VIC 3010, Australia*

Christopher J. Davis − *Vertex Pharmaceuticals (Europe), Ltd., Abingdon, Oxfordshire OX14 4RW, United Kingdom*

Katherine M. Wheelhouse − *Chemical Development, GSK Medicines Research Centre, Stevenage, Hertfordshire SG1 2NY, United Kingdom*

Complete contact information is available at: https://pubs.acs.org/10.1021/jacs.9b13260

Notes

The authors declare no competing financial interest.

■ ACKNOWLEDGMENTS

Richard Cooper (University of Oxford) is thanked for assistance with X-ray structure analysis, and Nader Amin and Tim Claridge (both University of Oxford) are thanked for assistance with NMR spectroscopy analysis. A.d.G. is grateful to the EPSRC Centre for Doctoral Training in Synthesis for Biology and Medicine (EP/L015838/1) for a studentship, and the generous support by GlaxoSmithKline, Vertex, AstraZeneca, Diamond Light Source, Defence Science and Technology Laboratory, Evotec, Janssen, Novartis, Pfizer, Syngenta, Takeda, and UCB is gratefully acknowledged.

■ REFERENCES

(1) Miyaura, N.; Yamada, K.; Suzuki, A. A New Stereospecific Cross-Coupling by the Palladium-Catalyzed Reaction of 1-Alkenylboranes with 1-Alkenyl or 1-Alkynyl Halides. *Tetrahedron Lett.* **1979**, *20*, 3437−3440.

(2) (a) Carey, J. S.; Laffan, D.; Thomson, C.; Williams, M. T. Analysis of the Reactions Used for the Preparation of Drug Candidate Molecules. *Org. Biomol. Chem.* **2006**, *4*, 2337−2347. (b) Brown, D. G.; Boström, J. Analysis of Past and Present Synthetic Methodologies on Medicinal Chemistry: Where Have All the New Reactions Gone? *J. Med. Chem.* **2016**, *59*, 4443−4458.

(3) Cox, P. A.; Leach, A. G.; Campbell, A. D.; Lloyd-Jones, G. C. Protodeboronation of Heteroaromatic, Vinyl, and Cyclopropyl Boronic Acids: pH-Rate Profiles, Autocatalysis, and Disproportionation. *J. Am. Chem. Soc.* **2016**, *138*, 9145−9157.

(4) Markovic, T.; Rocke, B. N.; Blakemore, D. C.; Mascitti, V.; Willis, M. C. Pyridine Sulfinates as General Nucleophilic Coupling Partners in Palladium-Catalyzed Cross-Coupling Reactions with Aryl Halides. *Chem. Sci.* **2017**, *8*, 4437−4442.

(5) Markovic, T.; Rocke, B. N.; Blakemore, D. C.; Mascitti, V.; Willis, M. C. Catalyst Selection Facilitates the Use of Heterocyclic Sulfinates as General Nucleophilic Coupling Partners in Palladium-Catalyzed Coupling Reactions. *Org. Lett.* **2017**, *19*, 6033−6035.

(6) Markovic, T.; Murray, P. R. D.; Rocke, B. N.; Shavnya, A.; Blakemore, D. C.; Willis, M. C. Heterocyclic Allylsulfones as Latent Heteroaryl Nucleophiles in Palladium-Catalyzed Cross-Coupling Reactions. *J. Am. Chem. Soc.* **2018**, *140*, 15916−15923.

(7) Ortgies, D. H.; Hassanpour, A.; Chen, F.; Woo, S.; Forgione, P. Desulfination as an Emerging Strategy in Palladium-Catalyzed C-C Coupling Reactions. *Eur. J. Org. Chem.* **2016**, *2016*, 408−425.

(8) Garves, K. Coupling, Carbonylation, and Vinylation Reactions of Aromatic Sulfinic Acids *via* Organopalladium Intermediates. *J. Org. Chem.* **1970**, *35*, 3273−3275.

(9) (a) Zhou, X.; Luo, J.; Liu, J.; Peng, S.; Deng, G.-J. Pd-Catalyzed Desulfitative Heck Coupling with Dioxygen as the Terminal Oxidant. *Org. Lett.* **2011**, *13*, 1432−1435. (b) Wang, G. W.; Miao, T. Palladium-Catalyzed Desulfitative Heck-Type Reaction of Aryl Sulfinic Acids with Alkenes. *Chem. - Eur. J.* **2011**, *17*, 5787−5790.

(10) Cheng, K.; Yu, H.-Z.; Zhao, B.; Hu, S.; Zhang, X.-M.; Qi, C. Palladium-Catalyzed Desulfitative Cross-Coupling of Arylsulfinates with Arylboronic Acids. *RSC Adv.* **2014**, *4*, 57923−57928.

(11) Cheng, K.; Hu, S.; Zhao, B.; Zhang, X. M.; Qi, C. Palladium-Catalyzed Hiyama-Type Cross-Coupling Reactions of Arenesulfinates with Organosilanes. *J. Org. Chem.* **2013**, *78*, 5022−5025.

(12) Sato, K.; Okoshi, T. Process for Producing Aromatic Compounds. U.S. Patent No. US5159082A, 1992.

(13) (a) Forgione, P.; Ortgies, D. A Ligand-Free Palladium-Catalyzed Cross-Coupling of Aryl Sulfinates with Aryl Bromides. *Synlett* **2013**, *24*, 1715−1721. (b) Zhou, C.; Liu, Q.; Li, Y.; Zhang, R.; Fu, X.; Duan, C. Palladium-Catalyzed Desulfitative Arylation by C-O Bond Cleavage of Aryl Triflates with Sodium Arylsulfinates. *J. Org. Chem.* **2012**, *77*, 10468−10472. (c) Zhou, C.; Li, Y.; Lu, Y.; Zhang, R.; Jin, K.; Fu, X.; Duan, C. Palladium-Catalyzed Desulfitative Cross-Coupling of Sodium Arylsulfinates with Aryl Bromides and Chlorides: An Alternative Convenient Synthesis of Biaryls. *Chin. J. Chem.* **2013**, *31*, 1269−1273. (d) Zhao, F.; Tan, Q.; Xiao, F.; Zhang, S.; Deng, G.-J. Palladium-Catalyzed Desulfitative Cross-Coupling Reaction of Sodium Sulfinates with Benzyl Chlorides. *Org. Lett.* **2013**, *15*, 1520−1523. (e) Forgione, P.; Ortgies, D.; Barthelme, A.; Aly, S.; Desharnais, B.; Rioux, S. Scope of the Desulfinylative Palladium-Catalyzed Cross-Coupling of Aryl Sulfinates with Aryl Bromides. *Synthesis* **2013**, *45*, 694−702.

(14) (a) Chen, W.; Li, P.; Miao, T.; Meng, L. G.; Wang, L. An Efficient Tandem Elimination-Cyclization-Desulfitative Arylation of 2-(Gem-Dibromovinyl)Phenols(Thiophenols) with Sodium Arylsulfinates. *Org. Biomol. Chem.* **2013**, *11*, 420−424. (b) Sévigny, S.; Forgione, P. Efficient Desulfinylative Cross-Coupling of Thiophene and Furan Sulfinates with Aryl Bromides in Aqueous Media. *New J. Chem.* **2013**, *37*, 589. (c) Colomb, J.; Billard, T. Palladium-Catalyzed

Desulfitative Arylation of 3-Haloquinolines with Arylsulfinates. *Tetrahedron Lett.* **2013**, *54*, 1471−1474. (d) Shi, J.; Tang, X.-D.; Wu, Y.-C.; Li, H.-N.; Song, L.-J.; Wang, Z.-Y. Palladium-Catalyzed Desulfitative Arylation of 5-Alkoxy-3,4-dibromo-2(5*H*)-furanone with Sodium Arylsulfinates. *Eur. J. Org. Chem.* **2015**, *2015*, 1193−1197. (e) Mangel, D.; Buonomano, C.; Sévigny, S.; Di Censo, G.; Thevendran, G.; Forgione, P. Efficient Desulfinative Cross-Coupling of Heteroaromatic Sulfinates with Aryl Triflate in Environmentally Friendly Protic Solvents. *Heterocycles* **2015**, *90*, 1228−1239.

(15) (a) Ortgies, D. H.; Chen, F.; Forgione, P. Palladium and TEMPO as Co-Catalysts in a Desulfinative Homocoupling Reaction. *Eur. J. Org. Chem.* **2014**, *2014*, 3917−3922. (b) Rao, B.; Zhang, W.; Hu, L.; Luo, M. Catalytic Desulfitative Homocoupling of Sodium Arylsulfinates in Water using $PdCl_2$ as the Recyclable Catalyst and O_2 as the Terminal Oxidant. *Green Chem.* **2012**, *14*, 3436−3440.

(16) Tanaka, D.; Romeril, S. P.; Myers, A. G. On the Mechanism of the Palladium(II)-Catalyzed Decarboxylative Olefination of Arene Carboxylic Acids. Crystallographic Characterization of Non-Phosphine Palladium(II) Intermediates and Observation of Their Stepwise Transformation in Heck-like Processes. *J. Am. Chem. Soc.* **2005**, *127*, 10323−10333.

(17) Zhang, S.-L.; Fu, Y.; Shang, R.; Guo, Q.-X.; Liu, L. Theoretical Analysis of Factors Controlling Pd-Catalyzed Decarboxylative Coupling of Carboxylic Acids with Olefins. *J. Am. Chem. Soc.* **2010**, *132*, 638−646.

(18) Adenot, A.; Char, J.; Von Wolff, N.; Lefevre, G.; Anthore-Dalion, L.; Cantat, T. SO_2 Conversion to Sulfones: Development and Mechanistic Insights of a Sulfonylative Hiyama Cross-Coupling. *Chem. Commun.* **2019**, *55*, 12924−12927.

(19) (a) Sraj, L. O. C.; Khairallah, G. N.; da Silva, G.; O'Hair, R. A. J. Who Wins: Pesci, Peters, or Deacon? Intrinsic Reactivity Orders for Organocuprate Formation *via* Ligand Decomposition. *Organometallics* **2012**, *31*, 1801−1807. (b) Skillinghaug, B.; Skold, C.; Rydfjord, J.; Svensson, F.; Behrends, M.; Savmarker, J.; Sjoberg, P. J.; Larhed, M. Palladium(II)-Catalyzed Desulfitative Synthesis of Aryl Ketones from Sodium Arylsulfinates and Nitriles: Scope, Limitations, and Mechanistic Studies. *J. Org. Chem.* **2014**, *79*, 12018−12032. (c) Behrends, M.; Sävmarker, J.; Sjöberg, P. J. R.; Larhed, M. Microwave-Assisted Palladium(II)-Catalyzed Synthesis of Aryl Ketones from Aryl Sulfinates and Direct ESI-MS Studies Thereof. *ACS Catal.* **2011**, *1*, 1455−1459.

(20) (a) Baskin, J. M.; Wang, Z. A Mild, Convenient Synthesis of Sulfinic Acid Salts and Sulfonamides from Alkyl and Aryl Halides. *Tetrahedron Lett.* **2002**, *43*, 8479−8483. (b) Emmett, E. J.; Hayter, B. R.; Willis, M. C. Palladium-Catalyzed Synthesis of Ammonium Sulfinates from Aryl Halides and a Sulfur Dioxide Surrogate: a Gas- and Reductant-Free Process. *Angew. Chem., Int. Ed.* **2014**, *53*, 10204−10208. (c) Kamiyama, T.; Enomoto, S.; Inoue, M. A Novel Synthesis of Aromatic Sulfinic Acids. *Chem. Pharm. Bull.* **1988**, *36*, 2652−2653. (d) Skillinghaug, B.; Rydfjord, J.; Odell, L. R. Synthesis of sodium aryl sulfinates from aryl bromides employing 1,4-diazabicyclo[2.2.2]octane bis(sulfur dioxide) adduct (DABSO) as a bench-stable, gas-free alternative to SO_2. *Tetrahedron Lett.* **2016**, *57*, 533−536.

(21) (a) Wei, C. S.; Davies, G. H.; Soltani, O.; Albrecht, J.; Gao, Q.; Pathirana, C.; Hsiao, Y.; Tummala, S.; Eastgate, M. D. The Impact of Palladium(II) Reduction Pathways on the Structure and Activity of Palladium(0) Catalysts. *Angew. Chem., Int. Ed.* **2013**, *52*, 5822−5826. (b) Amatore, C.; Jutand, A.; M'Barki, M. A. Evidence of the Formation of Zerovalent Palladium from $Pd(OAc)_2$ and Triphenylphosphine. *Organometallics* **1992**, *11*, 3009−3013. (c) Norton, D. M.; Mitchell, E. A.; Botros, N. R.; Jessop, P. G.; Baird, M. C. A superior precursor for palladium(0)-based cross-coupling and other catalytic reactions. *J. Org. Chem.* **2009**, *74*, 6674−80. (d) Li, H.; Grasa, G. A.; Colacot, J. A Highly Efficient, Practical, and General Route for the Synthesis of $(R_3P)_2Pd(0)$ Structural Evidence on the Reduction Mechanism of Pd(II) to Pd(0). *Org. Lett.* **2010**, *12*, 3332−3335.

(22) Amatore, C.; Jutand, A. Anionic Pd(0) and Pd(II) Intermediates in Palladium-Catalyzed Heck and Cross-Coupling Reactions. *Acc. Chem. Res.* **2000**, *33*, 314−321.

(23) Negishi, E.; Takahashi, T.; Akiyoshi, K. 'Bis-(tripheny1phosphine)palladium:' Its Generation, Characterization, and Reactions. *J. Chem. Soc., Chem. Commun.* **1986**, 1338−1339.

(24) Milstein, D.; Stille, J. K. Palladium-Catalyzed Coupling of Tetraorganotin Compounds with Aryl and Benzyl Halides. Synthetic Utility and Mechanism. *J. Am. Chem. Soc.* **1979**, *101*, 4992−4998.

(25) Steinhoff, B. A.; Stahl, S. S. Ligand-Modulated Palladium Oxidation Catalysis Mechanistic Insights into Aerobic Alcohol Oxidation with the $Pd(OAc)_2$ Pyridine Catalyst System. *Org. Lett.* **2002**, *4*, 4179−4181.

(26) (a) Louie, J.; Hartwig, J. F. A Route to Pd^0 from Pd^{II} Metallacycles in Animation and Cross-Coupling Chemistry. *Angew. Chem., Int. Ed. Engl.* **1996**, *35*, 2359−2361. (b) Strieter, E. R.; Blackmond, D. G.; Buchwald, S. L. Insights into the Origin of High Activity and Stability of Catalysts Derived from Bulky, Electron-Rich Monophosphinobiaryl Ligands in the Pd-Catalyzed C-N Bond Formation. *J. Am. Chem. Soc.* **2003**, *125*, 13978−13980.

(27) Huang, X.; Anderson, K. W.; Zim, D.; Jiang, L.; Klapars, A.; Buchwald, S. L. Expanding Pd-Catalyzed C−N Bond-Forming Processes: The First Amidation of Aryl Sulfonates, Aqueous Amination, and Complementarity with Cu-Catalyzed Reactions. *J. Am. Chem. Soc.* **2003**, *125*, 6653−6655.

(28) Thirupathi, N.; Amoroso, D.; Bell, A.; Protasiewicz, J. D. Reactivity Studies of Cationic Palladium(II) Phosphine Carboxylate Complexes with Lewis Bases; Substitution versus Cyclometalation. *Organometallics* **2007**, *26*, 3157−3166.

(29) Li, K.; Guzei, I. A.; Darkwa, J. Insertion of Sulfur Dioxide into Metal Carbon Bonds of Chloro(methyl)palladium Complexes. *Polyhedron* **2003**, *22*, 805−810.

(30) Shrestha, R.; Brennessel, W. W.; Weix, D. J. [2,2′-Bis-(diphenylphosphanyl)-1,1′-binaphthyl-[kappa]2P,P′]chlorido(4-methylphenylsulfonyl-[kappa]S)palladium(II) dichloromethane trisolvate monohydrate. *Acta Crystallogr., Sect. E: Struct. Rep. Online* **2011**, *67*, m1830.

(31) Higashi, L. S.; Lundeen, M.; Hilti, E.; Seff, K. Crystal and Molecular Structure of Bis(2-pyridine sulfinato)copper(II). *Inorg. Chem.* **1977**, *16*, 310−313.

(32) Mitchell, E. A.; Jessop, P. G.; Baird, M. C. A Kinetics Study of the Oxidative Addition of Bromobenzene to $Pd(PCy_3)_2$ (Cy = cyclohexyl) in a Nonpolar Medium: The Influence on Rates of Added PCy_3 and Bromide Ion. *Organometallics* **2009**, *28*, 6732−6738.

(33) Barrios-Landeros, F.; Carrow, B. P.; Hartwig, J. F. Effect of Ligand Steric Properties and Halide Identity on the Mechanism for Oxidative Addition of Haloarenes to Trialkylphosphine Pd(0) Complexes. *J. Am. Chem. Soc.* **2009**, *131*, 8141−8154.

(34) (a) Grushin, V. V.; Bensimon, C.; Alper, H. Dichlorobis-(tricyclohexylphosphine)palladium(II) Synthesis and Crystal Structure. An Exceptionally Simple and Efficient Preparation of Bis-(tricyclohexylphosphine)palladium(0). *Inorg. Chem.* **1994**, *33*, 4804−4806. (b) Stambuli, J. P.; Incarvito, C. D.; Bühl, M.; Hartwig, J. F. Synthesis, Structure, Theoretical Studies, and Ligand Exchange Reactions of Monomeric, T-Shaped Arylpalladium(II) Halide Complexes with an Additional, Weak Agostic Interaction. *J. Am. Chem. Soc.* **2004**, *126*, 1184−1194.

(35) (a) Lindsell, W. E.; Palmer, D. D.; Preston, P. N.; Rosair, G. M.; Jones, R. V. H.; Whitton, A. J. Investigations of Benzyl and Aryl Palladium Complexes with Pendant Hydroxy Substituents and Their Transformation into Benzolactones on Carbonylation. *Organometallics* **2005**, *24*, 1119−1133. (b) Hartwig, J. F. Transition Metal Catalyzed Synthesis of Arylamines and Aryl Ethers from Aryl Halides and Triflates: Scope and Mechanism. *Angew. Chem., Int. Ed.* **1998**, *37*, 2046−2067. (c) Widenhoefer, R. A.; Buchwald, S. L. Electronic Dependence of C−O Reductive Elimination from Palladium (Aryl)-neopentoxide Complexes. *J. Am. Chem. Soc.* **1998**, *120*, 6504−6511. (d) Widenhoefer, R. A.; Zhong, H. A.; Buchwald, S. L. Direct Observation of C−O Reductive Elimination from Palladium Aryl Alkoxide Complexes To Form Aryl Ethers. *J. Am. Chem. Soc.* **1997**, *119*, 6787−6795.

https://dx.doi.org/10.1021/jacs.9b13260
J. Am. Chem. Soc. 2020, 142, 3564−3576

(36) (a) Klinkenberg, J. L.; Hartwig, J. F. Slow Reductive Elimination from Arylpalladium Parent Amido Complexes. *J. Am. Chem. Soc.* **2010**, *132*, 11830−11833. (b) Arrechea, P. L.; Buchwald, S. L. Biaryl Phosphine Based Pd(II) Amido Complexes: The Effect of Ligand Structure on Reductive Elimination. *J. Am. Chem. Soc.* **2016**, *138*, 12486−12493.
(37) Alvaro, E.; Hartwig, J. F. Resting State and Elementary Steps of the Coupling of Aryl Halides with Thiols Catalyzed by Alkylbisphosphine Complexes of Palladium. *J. Am. Chem. Soc.* **2009**, *131*, 7858−7868.
(38) (a) Grushin, V. V.; Alper, H. Indirect Formation of Carboxylic Acids via Anhydrides in the Palladium-Catalyzed Hydroxycarbonylation of Aromatic Halides. *J. Am. Chem. Soc.* **1995**, *117*, 4305−4315. (b) Meyer, W. H.; Brüll, R.; Raubenheimer, H. G.; Thompson, C.; Kruger, G. J. Thioethercarboxylates in Palladium Chemistry: First Proof of Hemilabile Properties of S−O Ligands. *J. Organomet. Chem.* **1998**, *553*, 83−90.
(39) Shavnya, A.; Hesp, K. D.; Mascitti, V.; Smith, A. C. Palladium-Catalyzed Synthesis of (Hetero)Aryl Alkyl Sulfones from (Hetero)-Aryl Boronic Acids, Unactivated Alkyl Halides, and Potassium Metabisulfite. *Angew. Chem., Int. Ed.* **2015**, *54*, 13571−13575.
(40) Vitzthum, G.; Lindner, E. Sulfinato Complexes. *Angew. Chem., Int. Ed. Engl.* **1971**, *10*, 315−326.
(41) Cámpora, J.; López, J. A.; Palma, P.; del Rio, D.; Carmona, E.; Valerga, P.; Graiff, C.; Tiripicchio, A. Synthesis and Insertion Reactions of the Cyclometalated Palladium−Alkyl Complexes Pd-$(CH_2CMe_2$-*o*-$C_6H_4)L_2$. Observation of a Pentacoordinated Intermediate in the Insertion of SO_2. *Inorg. Chem.* **2001**, *40*, 4116−4126.
(42) (a) van Strijdonck, G. P. F.; Boele, M. D. K.; Kamer, P. C. J.; de Vries, J. G.; van Leeuwen, P. W. N. M. Fast Palladium Catalyzed Arylation of Alkenes Using Bulky Monodentate Phosphorus Ligands. *Eur. J. Inorg. Chem.* **1999**, *1999*, 1073−1076. (b) Sewell, L. J.; Huertos, M. A.; Dickinson, M. E.; Weller, A. S.; Lloyd-Jones, G. C. Dehydrocoupling of Dimethylamine Borane Catalyzed by Rh-$(PCy_3)_2H_2Cl$. *Inorg. Chem.* **2013**, *52*, 4509−4516. (c) Rosner, T.; Le Bars, J.; Pfaltz, A.; Blackmond, D. G. Kinetic Studies of Heck Coupling Reactions Using Palladacycle Catalysts: Experimental and Kinetic Modeling of the Role of Dimer Species. *J. Am. Chem. Soc.* **2001**, *123*, 1848−1855.
(43) (a) Marshall, J. E.; Keister, J. B.; Diver, S. T. Mechanism of Intermolecular Ene-yne Metathesis Promoted by the Grubbs First-Generation Catalyst: An Alternative Entry Point to Catalysis. *Organometallics* **2011**, *30*, 1319−1321. (b) Dias, E. L.; Nguyen, S. T.; Grubbs, R. H. Well-Defined Ruthenium Olefin Metathesis Catalysts: Mechanism and Activity. *J. Am. Chem. Soc.* **1997**, *119*, 3887−3897.
(44) Mitchell, E. A.; Baird, M. C. Optimization of Procedures for the Syntheses of Bisphosphinepalladium(0) Precursors for Suzuki−Miyaura and Similar Cross-Coupling Catalysis: Identification of 3:1 Coordination Compounds in Catalyst Mixtures Containing Pd(0), PCy_3, and/or P*Me*Bu_2. *Organometallics* **2007**, *26*, 5230−5238.
(45) (a) Brown, T. L.; Lee, K. J. Ligand Steric Properties. *Coord. Chem. Rev.* **1993**, *128*, 89−116. (b) Tolman, C. A. Steric Effects of Phosphorus Ligands in Organometallic Chemistry and Homogeneous Catalysis. *Chem. Rev.* **1977**, *77*, 313−348. (c) Wilson, M. R.; Woska, D. C.; Prock, A.; Giering, W. P. The Quantitative Analysis of Ligand Effects (QALE). The aryl effect. *Organometallics* **1993**, *12*, 1742−1752.
(46) (a) An, Y.; Xia, H.; Wu, J. A Palladium-Catalyzed Coupling Reaction of Aryl Nonaflates, Sulfur Dioxide, and Hydrazines. *Org. Biomol. Chem.* **2016**, *14*, 1665−1669. (b) Davies, A. T.; Curto, J. M.; Bagley, S. W.; Willis, M. C. One-Pot Palladium-Catalyzed Synthesis of Sulfonyl Fluorides from Aryl Bromides. *Chem. Sci.* **2017**, *8*, 1233−1237. (c) Nguyen, B.; Emmett, E. J.; Willis, M. C. Palladium-Catalyzed Aminosulfonylation of Aryl Halides. *J. Am. Chem. Soc.* **2010**, *132*, 16372−16373. (d) Richards-Taylor, C. S.; Blakemore, D. C.; Willis, M. C. One-Pot Three-Component Sulfone Synthesis Exploiting Palladium-Catalysed Aryl Halide Aminosulfonylation. *Chem. Sci.* **2014**, *5*, 222−228. (e) Shavnya, A.; Coffey, S. B.; Smith, A. C.; Mascitti, V. Palladium-Catalyzed Sulfination of Aryl and Heteroaryl Halides: Direct Access to Sulfones and Sulfonamides. *Org. Lett.* **2013**, *15*, 6226−6229. (f) Ye, S.; Wu, J. A Palladium-Catalyzed Reaction of Aryl Halides, Potassium Metabisulfite, and Hydrazines. *Chem. Commun.* **2012**, *48*, 10037−10039.
(47) Kimura, S.; Smith, J. M. Kinetics of the Sodium Carbonate−Sulfur dioxide Reaction. *AIChE J.* **1987**, *33*, 1522−1532.
(48) (a) Anthony, E. J.; Granatstein, D. L. Sulfation Phenomena in Fluidized Bed Combustion Systems. *Prog. Energy Combust. Sci.* **2001**, *27*, 215−236. (b) Wappel, D.; Joswig, S.; Khan, A. A.; Smith, K. H.; Kentish, S. E.; Shallcross, D. C.; Stevens, G. W. The Solubility of Sulfur Dioxide and Carbon Dioxide in an Aqueous Solution of Potassium Carbonate. *Int. J. Greenhouse Gas Control* **2011**, *5*, 1454−1459.
(49) Arroniz, C.; Denis, J. G.; Ironmonger, A.; Rassias, G.; Larrosa, I. An Organic Cation as a Silver(I) analogue for the Arylation of sp^2 and sp^3 C−H Bonds with Iodoarenes. *Chem. Sci.* **2014**, *5*, 3509−3514.
(50) (a) Benson, S. W. III - Bond energies. *J. Chem. Educ.* **1965**, *42*, 502. (b) Kerr, J. A. Bond Dissociation Energies by Kinetic Methods. *Chem. Rev.* **1966**, *66*, 465−500.
(51) Beccalli, E. M.; Broggini, G.; Martinelli, M.; Sottocornola, S. C−C, C−O, C−N Bond Formation on sp^2 Carbon by Pd(II)-Catalyzed Reactions Involving Oxidant Agents. *Chem. Rev.* **2007**, *107*, 5318−5365.

https://dx.doi.org/10.1021/jacs.9b13260
J. Am. Chem. Soc. 2020, 142, 3564−3576